Interaction between gravity waves and a shear flow

By B. A. HUGHES* AND R. W. STEWART
Institute of Oceanography and Department of Physics, University of British Columbia, Vancouver 8, B.C.

(Received 17 September 1960)

A series of experiments has been undertaken in which three major properties of a surface tension-gravity wave system have been examined. The results of these experiments have been compared with existing theories. The three properties are: (i) viscous decay in the absence of mean flow, the relevant theory being given in Lamb (1932, § 348); (ii) propagation velocities in the presence and absence of flow (Lamb 1932, § 267), and (iii) the change of wave energy on crossing a stable Couette shear flow. The measurements in the last case were compared with two theories, one obtained from the Navier–Stokes equations including terms up to second order in wave slope, the other, following previous authors, obtained on the assumption that any direct interaction of the waves with the shear flow is negligible. According to the theory obtained from the Navier–Stokes equations, the divergence of surface wave energy is equal to the rate of change of wave energy due to the interaction between the mean flow and the wave system plus the rate of change of wave energy due to viscous decay.

An optical system was used to measure the maximum wave slopes, the wave-numbers and the shear velocities.

Results indicate that an anomalous region of wave properties exists for wave-numbers near 2·7 cm^{-1}. For a set of data in which the wave-numbers were always less than 1·8 cm^{-1}, it was found that the viscous decay rate and the propagation laws agree with theory to within the experimental error, and the interaction measurements fit the theory with the non-linear term included rather than the traditional theories.

1. Introduction

The work discussed herein is an experimental investigation of three major properties of deep water surface waves in the régime where both surface tension and gravity are important. These properties are: viscous dissipation in the absence of any mean flow, propagation laws in the presence and absence of mean flow, and the non-linear interaction of waves with a horizontal mean shear. The first two of these are treated theoretically in Lamb (1932). The last has been investigated theoretically by Longuet-Higgins & Stewart (1961), and in a special case by Drent (1959).

The analysis given by Drent is for the case of plane, long crested waves and a rectilinear shear flow in the absence of surface tension and viscosity. The results

* Now at Pacific Naval Laboratory, H.M.C. Dockyard, Esquimalt, B.C.

indicate that there are two major causes of amplitude change as the waves traverse the flow: one is due to the refraction of the waves, causing a spreading or concentration of energy; the other is due to the radiation pressure, associated with the waves, interacting directly with the shear flow. For waves running directly into a converging flow, these two effects are about equal; for waves crossing a lateral shear at an angle, the former appears to be two to three times larger than the latter. Previous discussions have consistently neglected the direct interaction effects (for example, Johnson 1947), which are of the same nature as those treated recently by Longuet-Higgins & Stewart (1960, 1961).

This paper describes a laboratory experiment designed to measure the three properties listed above and a comparison of the results with the respective theoretical predictions. The wave-energy measurements in the presence of mean flow are compared with two theoretical models—one including the interaction effects, and the other omitting the interaction effects.

2. Experimental methods

Flow production

All experiments were carried out in a tank specially constructed to produce the required shear flow.

A stable, cylindrical Couette flow was created between the outer wall of a circular tank slightly greater than 2·5 m in diameter and an inner wall imposed by a raised centre portion 1·52 m in diameter (figure 1). A hollow annular ring, 2·44 m in diameter, floating freely, was concentric with and about 2·5 cm radially inside the outer wall of the circular tank (figure 1). A series of six drive jets situated in the outer wall of the tank were connected by rubber hoses to the water mains (figure 1). These jets were oriented so that water passing through them impinged on the wall of the annular ring at an angle of 45°, thereby making it rotate. In order to keep the annular ring rotating about the centre of the tank, three foam-padded castors, spring-mounted, were situated on the wall of the tank to bear gently on the outside of the rotating ring if it were not in the centre of the system (figure 1). It was found that if these castors were not used, the ring gradually shifted its axis of rotation until it hit the wall of the tank, creating a large disturbance on the surface of the water. It was necessary to construct a wooden form to fit snugly around the annular ring in order to hold it to a circular shape (figure 1). With the wooden form, the annular ring was circular to within 0·6 cm in its 2·44 m diameter.

Wave production

The device used to produce the waves consisted of a wooden truncated circular cone 1·9 cm deep with an upper diameter of 15·2 cm tapering to a lower diameter of 11·5 cm. It was firmly attached to the cone of a Jensen no. B 69 V elliptical loudspeaker. This assembly was situated on the top of the raised centre piece of the tank in such a way that excursions of the cone were perpendicular to the surface of the water. The cone extended about 1 cm under the surface.

The loudspeaker was driven by a low-frequency oscillator through a rotating switch (for pulse production) and a matching transformer. The voltage applied

to the wave-maker was continuously monitored by a single-beam oscilloscope. The performance of the oscillator was checked by a precision counter and its frequency found to be stable, over the time intervals of interest, to better than one part per thousand. The actual frequencies employed were measured either by use of a stop-watch or by comparison with the 60-cycle mains. (The mains frequency in the power grid to which we are connected, controlled at Boulder Dam, is noted for stability and accuracy.)

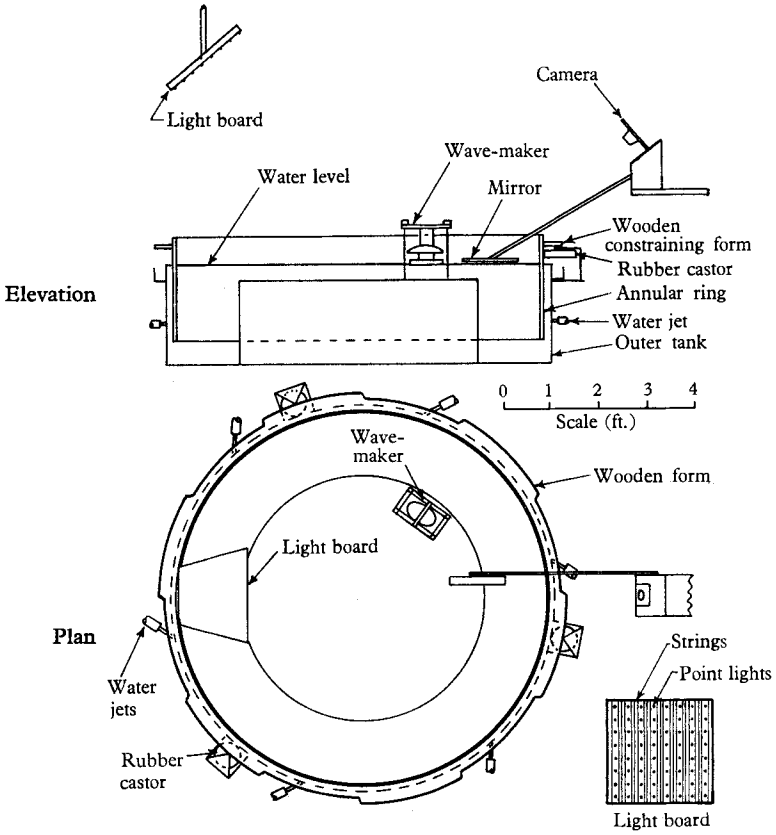

FIGURE 1. Experimental apparatus.

As in any experiment with waves, it was necessary to choose between an efficient wave absorber and the use of pulse techniques. No simple efficient absorber seemed compatible with the other requirements of the experiment, so a pulse system was adopted. Pulses of 10 sec duration at 1 min intervals were found to be reasonably satisfactory in eliminating disturbances due to reflected waves.

Two of the prime difficulties of wave production by this method arise from lobal pattern asymmetry and transient modulation. Asymmetry occurs because of the difficulty of properly orienting the wooden disk with respect to the water. It appears that the bottom of the disk should be accurately parallel to the surface of the water, and that the motion of the disk should be accurately perpendicular to it. Transient modulation occurs because a resonant system is driven by pulses of off-resonance frequency, and because an impulsive type of motion is imparted

to the surface of the water at the start of the pulse. Even though the voltage amplitude on the oscilloscope is constant to within 1 % there still is evidence of a transient modulation of 2–5 % in the waves themselves. A reduction of the effect of this modulation was obtained by averaging the results of amplitude measurements taken at a different stage of each of a large number of pulses.

Measurement of mean flow

Measurement of the horizontal shear-flow profiles was performed photographically during the experiment in the following way: ten circular pieces of white paper 0·6 cm in diameter were simultaneously dropped onto the surface of the water in a line approximately at right angles to the flow in the area under consideration. A photograph was taken of these with the camera shutter open for 0·98 sec (1 sec on camera settings). The lengths of the resulting streaks on the film are proportional to the speeds at the points where the pieces of paper were dropped. This was done ten times in order to achieve a smooth profile.

Visual observations of the vertical velocity profile were obtained by comparing the flow at a few cm depth and the flow right on the surface. A small plastic float about $\frac{1}{2}$ cm in diameter was attached to a relatively high drag body of about the same dimensions by a piece of thread a few cm long. The rate of movement of this unit when placed in the water was found to be not significantly different from the rate of movement of a plastic float by itself at the same radius. There is little reason to believe that an appreciable surface stress exists, so any depth-wise velocity gradient would be associated with secondary flow.

Such a secondary flow must of course exist. The stationary bottom of the tank must have associated with it an inward-flowing boundary layer. A compensating outward flow is thus required in the upper regions of the flow. If all the vertical movement occurs at the inner and outer walls of the tank, then in the main body of the annulus, solution of the vorticity equation yields for the tangential velocity V

$$V = B(r^n - r_0^{n+1} r^{-1}), \tag{1}$$

with B and n undetermined constants and r_0 the radius of the inner wall. The smooth curves shown in figures 2 and 3 were obtained by an empirical fit of equation (1) to the measured points. The velocity values used in the various calculations were taken from the theoretical curves (except in figure 3 for a distance less than 85 cm for which values were taken from the visually smoothed experimental data).

According to the above assumptions, the speed of the secondary flow is given by $(n-1)\nu/r$. With values of n obtained from the empirical fit this appears to be of the order of 10^{-4} cm/sec. The strength of the secondary flow was examined experimentally by observing the trajectories of the small plastic floats described above. These were somewhat irregular, but the trend was towards the outer wall, with a rate of radial progression estimated to be of the order of $\frac{1}{200}$ or less of the average tangential flow.

It should be noted that our results do not depend upon the accuracy of the assumptions leading to (1), since in practice the equation has been used merely as a framework for an empirical description of the mean velocity data.

Wave measurement

An optical system was used to measure the wave amplitudes, wave-number and wave direction. A board containing 64 light bulbs was fastened to the ceiling so that the light from these effective point sources reflected off the area of the shear

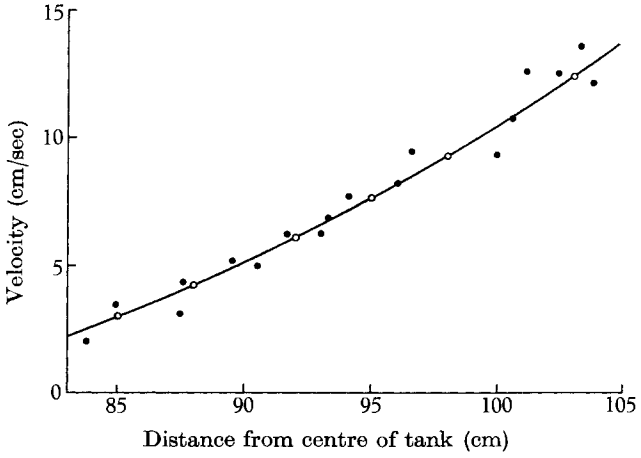

FIGURE 2. Velocity profile used for set I data. The 'theoretical' curve is obtained from equation (1) with empirically chosen constants. ○, Theoretical; ●, measured.

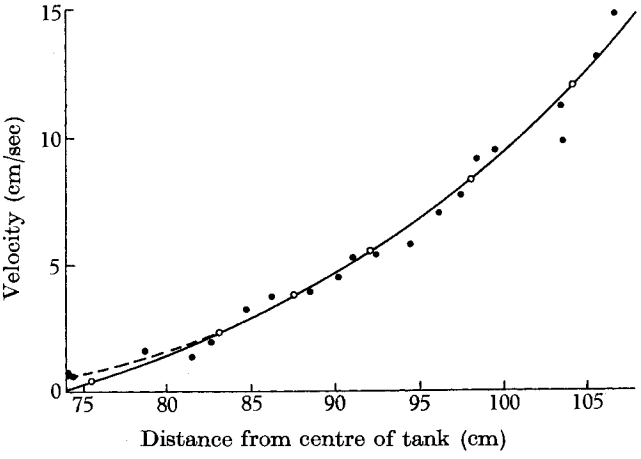

FIGURE 3. Velocity profile used for set II data. – – – –, Smoothed experimental data; —, theoretical curve.

flow to be studied into a properly oriented camera. The lights were in a square array each 7·6 cm apart. The board was approximately 3 m vertically above the surface of the water and approximately 3 m horizontally from the reflexion points on the surface of the water (figure 1). The camera used was a 35 mm Agfa Colorflex. It was positioned approximately 1 m vertically and horizontally from the reflexion points on the water surface, and angled so that the image of the 'light board' appeared in the centre of its field of view.

(i) *Amplitude*

As the waves cross the image of the board, the image of a light undergoes oscillatory excursions, the maximum of which is a direct measure of the maximum wave slope at the position on the surface of the water from which the undeviated light reflects. For each pulse the camera shutter was opened for somewhat longer than one wave period. The lengths of the streaks thus obtained on each frame are a measure of the maximum excursions of the images of the lights. A small alignment mirror, mounted just above the surface of the water and to one side of the image of the light board, was oriented to reflect one column of lights into the camera thus producing a constant reference line from frame to frame. (Examples of these photographs are given in figures 4*a* and 4*b*, plate 1.) The sensitivity of this technique is such that wave slopes of only 0·01 radians could be measured to within 1 %. The fact that the experimental waves had such small slopes justifies the use of first-order wave theory throughout.

(ii) *Wave-number*

The light board also has 23 straight white nylon strings mounted on it, each in a vertical plane (figure 1). These strings were photographed using an electronic flash unit. (Examples of these photographs are also shown in figures 4*c* and 4*d*, plate 2.)

As the waves cross the area in question, the images of the strings distort into sinusoids. Lines of constant phase were determined from photographs of this nature as follows: a photograph was first taken of the strings with no surface waves in the area, then photographs were taken when waves were present. When the first photograph was projected, the images of the straight strings were traced onto a piece of graph paper on the projection board and the images of the lights in the alignment mirror were traced out.* Then the photographs with waves were projected onto this same piece of graph paper. When the images of the lights in the alignment mirror correspond with the traced images, the traces of the straight strings form a baseline for each of the sinusoidal string images. The positions at which each sinusoidal image crossed its baseline were marked. Joining these marks along wave fronts then produced lines of constant phase.

(iii) *Projection system*

In order to facilitate measurement of the data on the films, a tilted board projection system was used with the focal length of the projector the same as the focal length of the camera. If the board onto which the film is projected is tilted with respect to the projector to the same angle as the surface of the water makes with the camera, the measurements obtained correspond directly to the plane of the surface of the water, to within a uniform scale factor.

* Because of the high contrast of the positive, the positions of the lights in the alignment mirror are not visible in figures 4*c* and 4*d*. They could be clearly seen, however, in the projected negatives.

3. Propagation in the absence of mean flow

Wave-number

Assuming irrotationality, incompressibility and infinitesimally small amplitudes, the phase velocity C for surface waves can be shown to be (Lamb, 1932, §267)

$$C = \left(\frac{g}{k} + \frac{kT}{\rho}\right)^{\frac{1}{2}}, \tag{2}$$

where T is the surface tension and k is the radian wave-number.

T was measured by observing the rise in a capillary tube of known bore, and found to be 67 ± 4 dynes/cm.

For a wave frequency of 8·00 c/s, the predicted wave-number is therefore

$$k_t = 2{\cdot}015 \pm 0{\cdot}02 \text{ cm}^{-1}.$$

Two experimental determinations at this frequency gave

$$k_e = 2{\cdot}028 \pm 0{\cdot}02 \text{ cm}^{-1}$$

and $$2{\cdot}033 \pm 0{\cdot}02 \text{ cm}^{-1}.$$

It therefore appears that the theory is at least as reliable as the measurements (i.e. ± 1 %) for small amplitude waves at this frequency.

Viscous dissipation

It is shown in Lamb (1932, §348) that if the motion in real waves is not significantly different from that in irrotational waves, then the expression for the amplitude a of plane waves as a function of time t is

$$a = a_0 e^{-2\nu k^2 t}, \tag{3}$$

where ν is the kinematic viscosity.

In terms of the parameters measured in our experiment, where we have cylindrically expanding waves, this becomes

$$\delta = \delta_0 (s_0/s)^{\frac{1}{2}} \exp\{-2\nu k^2 (s - s_0)/C_g\}, \tag{4}$$

where δ is the wave slope,

s is the distance from the centre of the wave-maker, and

C_g is the group velocity, which is taken as

$$C_g = \partial(kC)/\partial k, \tag{5}$$

where C is given by (2).

In practice the rate of dissipation of wave energy is changed severely by the presence of a surface film of oil or other immiscible surface material. Experience showed that the film must be continuous over dimensions comparable with a wavelength to be effective. Thus it was found that by slowly siphoning off surface water, and with it the surface film, the water could be kept adequately clean without requiring many special precautions to prevent contamination. The only essential was that the siphon draw off both air and water to ensure that the interfacial surface be carried away.

Viscosity was not measured. However, an examination of tabulated values shows that it is very insensitive to concentrations of solutes as dilute as are found in tap-water. The temperature of the surface water was measured and the viscosity taken from the *Handbook of Chemistry and Physics*, 41st ed., Chemical Rubber Publishing Co., Cleveland.

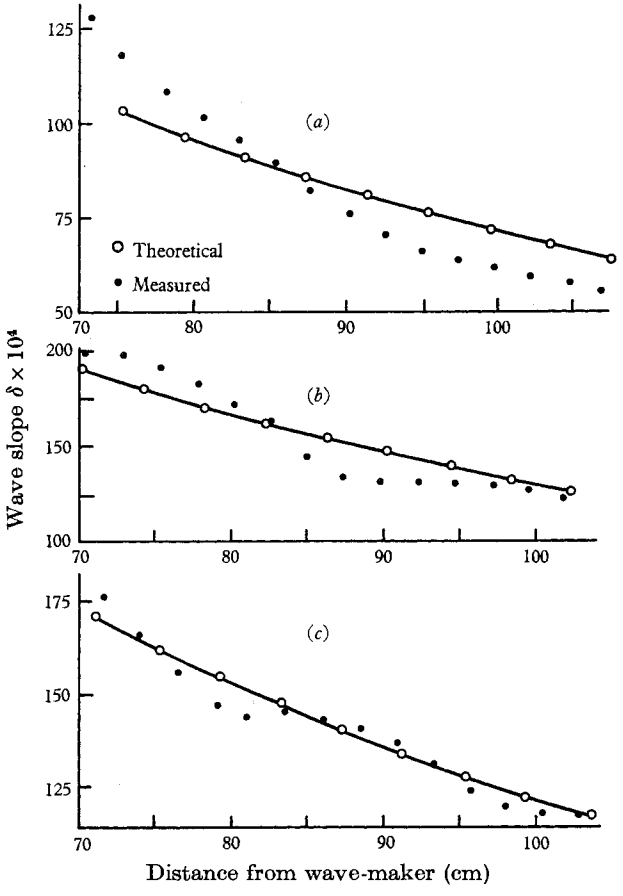

FIGURE 5. Viscous dissipation. ●, Experimental points; ○—○, theoretical line. (*a*) $f = 10{\cdot}00$ c/s, $k = 2{\cdot}69$ cm^{-1}; (*b*) $f = 8{\cdot}57$ c/s, $k = 2.21$ cm^{-1}; (*c*) $f = 8{\cdot}00$ c/s, $k = 2{\cdot}02$ cm.$^{-1}$

Figure 5 shows values of δ observed for frequencies of 8·00, 8·57 and 10·00 c/s, plotted as a function of s. The solid lines are obtained from equation (4). Since there is no preferred assignment to δ_0, the theoretical lines have been made to fit the experimental data near the centre of the range.

The 8·00 c/s data are seen to agree quite well with the theory except for the wavy characteristic of the measured points. This waviness is thought to be due to the presence of small amounts of reflected energy.

At 8·57 c/s the agreement is less satisfactory, but the observations cannot be said to conflict significantly with the theory.

The 10·0 c/s data were taken with the aim of measuring the viscous dissipation of a wave whose phase velocity is exactly the same as that of a wave twice its

frequency. Unfortunately, it appears that this condition has not been achieved. From the photographs used to measure the wave slopes it could be seen that an extra wave train was present, but in the distance covered by the measurements the phase of this extra wave with respect to the 10·0 c/s wave changed by 90°. It is thought that the apparently rapid decay over the left side of the graph in figure 5 is a combination of two factors. One is the fact that any wave of a frequency of 20·0 c/s which has appreciable amplitude that far from the wave-maker must have a continuous source of energy as it propagates. The only apparent source of energy is a non-linear wave-wave interaction with the 10·0 c/s wave. Between any crest of the fundamental and the preceding trough there is a region which is undergoing a continual rate of compression by the fluid particle velocities. If a part of an extra wave happens to coincide with this region for any length of time it will be increased in energy by the same sort of interaction as that between waves and a mean shear (Longuet-Higgins & Stewart 1960). The larger velocity gradients present in the 20·0 c/s wave result in a much faster decay of energy to viscosity; so presumably a balance is achieved between non-linear input and viscous decay. The 10·0 c/s wave thus experiences an increased rate of loss of energy through the intermediary of the 20·0 c/s wave. A phase photograph of a wave at 10·5 c/s is given in figure 4*d*, plate 2, clearly showing the complexity of the wave form when the frequency is near 10 c/s.

The other factor contributing to the anomalous measured decay rate of the 10·0 c/s waves is due to the change of phase that occurs between the two wave trains. The shape of the parts of the wave from which the light reflexions take place can be inferred from the character of the streak density obtained from an amplitude photograph. From such an examination it appears that the parts of the wave which give the maximum excursions of the reflected light change from having a slope more nearly like that of 20·0 c/s to that characteristic of a 10·0 c/s saw-tooth wave.

The peculiarities of waves in the neighbourhood of 10 c/s have been noted previously (Wilton 1915, Pierson & Fife 1960).

4. Wave-shear flow interaction

Drent's (1959) treatment was for a plane shear flow traversed by waves which would be straight-crested in any region where the shear was zero. Our case, while not different in principle, is more complex because we have a curved shear flow and a point source of waves.

Wave kinematics

The direction of phase propagation and the local wave-number are governed by two equations. The first is simply an expression of the fact that to an observer stationary relative to the wave-maker, the rate of change of phase is constant at all positions in the field. Thus

$$\omega_0 = kC - kV\sin\phi, \tag{6}$$

where ω_0 is the radian frequency at the wave-maker,

V is the local speed of the current,

and ϕ is the angle between the direction of the local wave front and the direction of the current velocity.

The second describes the refraction of the wave front. If η is a co-ordinate along a wave front and ξ a co-ordinate normal to it in the direction of propagation, then

$$(C - V\sin\phi)\frac{\partial\phi}{\partial\xi} = \frac{\partial C}{\partial\eta} - \frac{\partial}{\partial\eta}(V\sin\phi). \tag{7}$$

The rather complex relation (2) between C and k, together with the difficult semi-empirical form for V, (1), makes analytic treatment of these equations (6) and (7) formidable. However, in practice it was always found possible to work in a region where C, k and ϕ were all nearly independent of θ, the angular co-ordinate of a cylindrical co-ordinate system with centre at the centre of the tank. In this case an iterative successive approximation method permitted 'phase rays', defined everywhere by the direction of the vector sum of **C** and **V**, to be located without undue difficulty. The same calculation gives k and ϕ throughout the field.

Using the cylindrical co-ordinate system, equation (7) becomes

$$\cos\phi\frac{\partial\phi}{\partial r} - \sin\phi\frac{\partial\phi}{\partial\theta} + \frac{\sin\phi}{r} = -\sin\phi\frac{\partial\ln k}{\partial r} - \cos\phi\frac{\partial\ln k}{\partial r}. \tag{8}$$

Under the assumption that k and ϕ are independent of θ, this can be integrated to give

$$kr\sin\phi = k_0 L, \tag{9}$$

where k_0 is the wave-number at the wave-maker and L is the distance from the centre of the tank to the wave-maker. From equations (9) and (6), $\sin\phi$ is eliminated, leaving k as a function of r only,

$$kC - \omega_0 = k_0 VL/r. \tag{10}$$

Equation (6) can be used to estimate the accuracy of (10) using $\partial\phi/\partial\theta$ as evaluated in the absence of flow. This indicates that in the area investigated k is nowhere different from that given in (10) by more than 0·5 %.

Measurements of wave-number variation were obtained from two independent sets of data in the presence of flow: set I with an oscillator frequency of 8·23 c/s and a velocity profile as shown in figure 2, set II with an oscillator frequency of 6·00 c/s and a velocity profile as shown in figure 3.

For set I, a total of 40 wave-number pictures were taken of which 5 were chosen and measured. Judgement was based on the visual smoothness of the sinusoidal string images. Lack of smoothness results partially from velocity fluctuations and predominantly from the presence of any waves of a period different from the main component. Equations (6) and (8) indicate that waves of different period refract differently, thus the presence of spurious wave periods produces local variations along the lines of constant phase.

For set II, an attempt was made to take forty photographs but because of a faulty camera aperture mechanism only ten usable ones resulted. On the whole, these ten were much freer from discrepancies than those of set I so that no difficulty was encountered in choosing five frames.

Figures 6 and 7 contain typical lines of constant phase taken from data from two of each of the five frames of sets I and II, respectively.

The theoretical curves shown in figures 8 and 9 were plotted from equation (10) and were determined from set I information and set II information, respectively. The measured points were derived from the wavelengths obtained from the respective lines-of-constant-phase diagrams. The values used for the wavelengths

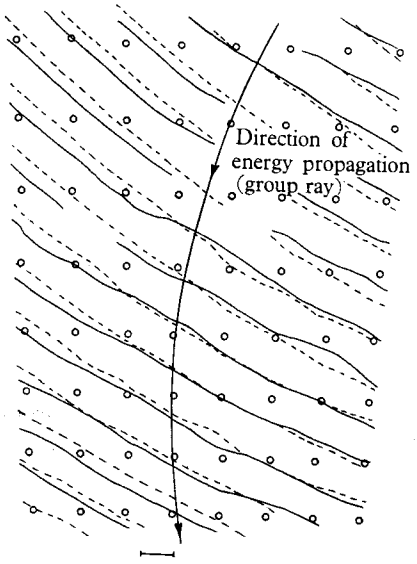

FIGURE 6. Lines of constant phase—set I (8·23 c/s). The circles are the average location of the images of lights used for amplitude measurement.

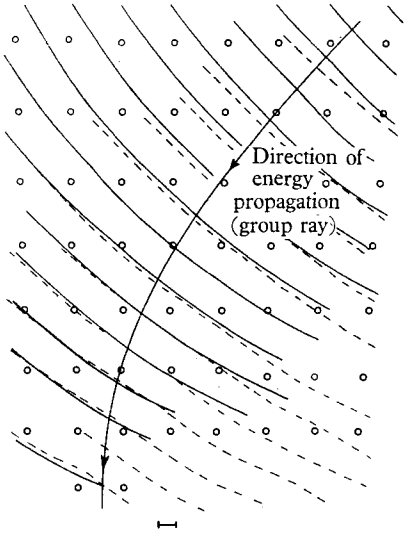

FIGURE 7. Lines of constant phase—set II (6·00 c/s).

are the averages, at each position, of the minimum distance from a point on a line of constant phase to the nearest lines of the same phase in both directions. In order to show the scatter yet not overcrowd the diagrams, only $\frac{1}{35}$ of all the points, chosen randomly, have been shown in each case. Smoothing of the measured points in figure 8 was done visually.

As can be seen from figures 8 and 9, set II data agree very well with equation (10) whereas set I differs significantly from it. The maximum discrepancy in figure 8 (approximately 5 %) occurs at $k = 2{\cdot}7\ \mathrm{cm}^{-1}$, and since the wave-number that propagates at the same phase velocity as a wave at twice the wave-number has a value of $2{\cdot}7\ \mathrm{cm}^{-1}$, calculated from equation (2), it is thought that the two phenomena are intimately linked, though exactly how is not yet understood. The most likely possibility is that the phase velocity in the vicinity of $k = 2{\cdot}7\ \mathrm{cm}^{-1}$ differs from that given by simple theory (equation 2) by approximately 5 %.

Interaction dynamics

(i) *Theory*

Longuet-Higgins and Stewart (1961) have shown that for steady currents and in the absence of wave dissipation

$$\nabla.[E(\mathbf{C}_g + \mathbf{U})] + \tfrac{1}{2}S_{ij}\left(\frac{\partial U_i}{\partial x_j} + \frac{\partial U_j}{\partial x_i}\right) = 0, \tag{11}$$

where E is wave energy per unit surface area,

$\mathbf{C}_g$ is the local group velocity of the waves,

$\mathbf{U}$ is the horizontal current velocity, of which

U_i is a component,

S_{ij} is the (two-dimensional) radiation stress-tensor.

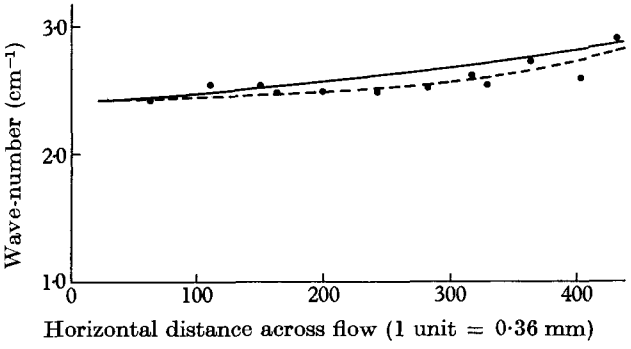

FIGURE 8. Measured and predicted wave-number data—set I (8·23 c/s). ●, Measured points; – – – –, smoothed experimental data; —, theoretical curve.

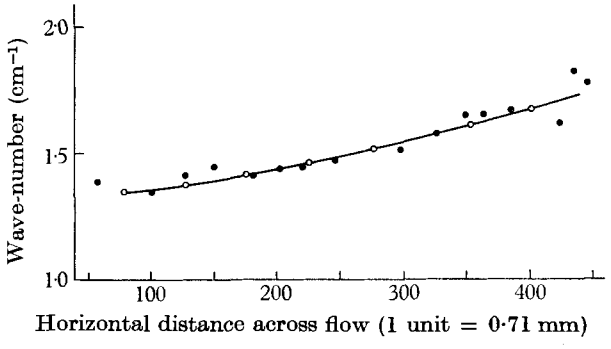

FIGURE 9. Measured and predicted wave-number data—set II (6·00 c/s). ●, Measured points; ○, theoretical curve.

In deep water the diagonal form of S_{ij} is

$$S_{ij} = \begin{pmatrix} \frac{1}{2}E & 0 \\ 0 & 0 \end{pmatrix}, \tag{12}$$

where the x_1 co-ordinate is here directed normal to the wave fronts.

Drent (1959) and Longuet-Higgins & Stewart (1961) analysed (11) for the particular case

$$\frac{\partial E}{\partial x_2} = \frac{\partial C}{\partial x_2} = \frac{\partial U_2}{\partial x_2} = U_1 = 0,$$

but previous authors (e.g. Johnson, 1947) have neglected the interaction term in S_{ij}.

In our case (11) becomes

$$\nabla.[E(\mathbf{C}_g + \mathbf{V})] = \tfrac{1}{4}E \sin 2\phi \left(\frac{\partial V}{\partial r} - \frac{V}{r}\right) - \text{viscous term}, \tag{13}$$

where $\mathbf{C}_g$ is in the direction of advance of the wave and normal to its front, and $\mathbf{V}$ is tangential to the mean streamline and in the direction of increasing θ.

The line obtained by integrating from the inner edge of the flow outwards with the direction of $\mathbf{C}_g + \mathbf{V}$, (a function of r and θ), tangent at every point to the path, shall be called a 'group ray'. A path line defined this way possesses the property that no wave energy crosses it. That is, given any two group rays, the rate that energy flows across any line joining these rays is the same as the rate that energy flows across any other line joining them in the absence of dissipating mechanisms and non-linear interactions. Therefore, by considering the configuration of the group rays on the water surface, the effect of the refraction and spreading of energy can be taken into account.

We shall assume that the effect of viscosity on the waves, being a purely local one, is not influenced by the shear flow and is given by (3) in the form

$$\left(\frac{dE}{ds}\right)_{\text{viscous}} = \frac{-4\nu k^2 E}{|\mathbf{C}_g + \mathbf{U}|}, \tag{14}$$

where s is the distance from the wave maker here measured along the local group ray.

Equation (13) can be put in a form suitable for numerical iteration by integrating it over the area contained between two differentially separated group rays and any two arbitrary points on the rays

$$E_2|\mathbf{C}_g + \mathbf{V}|_2 l_2 - E_1|\mathbf{C}_g + \mathbf{V}|_1 l_1 = \frac{1}{4}\int\int_1^2 E \sin 2\phi \left(\frac{dV}{dr} - \frac{V}{r}\right) dl\, ds - \text{viscous terms}, \tag{15}$$

or

$$\frac{\Delta(E|\mathbf{C}_g + \mathbf{V}|\, l)}{l\Delta s} = \tfrac{1}{4} \sin 2\phi \left(\frac{dV}{dr} - \frac{V}{r}\right) - \text{viscous terms}, \tag{16}$$

where l is the perpendicular distance separating the two group rays and Δs is an element of length along the group rays.

The theoretical curves used for comparison with the experimentally determined data have been obtained by a numerical integration of equation (16), including viscosity, along a previously determined group ray—the interaction curve including the term $\frac{1}{4}E \sin 2\phi(dV/dr - V/r)$, the non-interaction curve omitting it.

(ii) *Results*

For both sets of data, 100 amplitude photographs were taken and the 'best' twenty in each were measured. The criterion used to judge which frames were to be measured was based on overall smoothness of the streak lengths within the frame being judged. (See figures 4*a* and 4*b*, plate 1, for an example of a photograph rejected on this basis compared with one that was not.) The judgement was a purely visual one, i.e. it was performed before any of the streak lengths were actually measured. These anomalous streak variations are caused by the accumulative effect of fluctuations in the horizontal velocity that occur during the time required for the energy to propagate from the edge of the shear flow to the position of examination. The major effect of a local velocity fluctuation is a change of the rate of spreading from that point onwards along the group rays affected.

To determine the results of the interaction measurements a group ray was first plotted along which equation (16) was solved numerically with and without the interaction term. The group rays that were used were obtained simply from a graphical integration of the equation

$$-r\frac{d\theta}{dr} = \tan\phi - \frac{V}{C_g}\sec\phi, \tag{17}$$

where C_g is obtained from equation (5), assuming (2). The angle ϕ was in all cases determined from equation (10) using the measured values of k and V. The group rays so obtained are shown in figures 6 and 7, for set I and II, respectively. Eight wave slopes were then determined for each frame of amplitude photographs chosen to be measured—one for each row of lights. If the group ray happens to pass between two lights, the value of the slope at the ray was obtained by linear

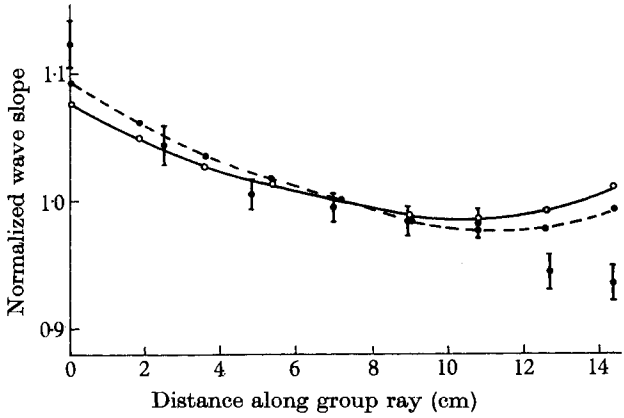

FIGURE 10. Wave slopes in presence of flow—set I (8·23 c/s). ○, Theoretical interaction; ●, theoretical non-interaction; ⧳, measured ± 1 S.E.

interpolation between the lights. Each frame was then normalized by setting the average wave slope along the group ray for each frame to unity. The normalized measured values for each point on the group ray were then averaged over all twenty frames. The standard errors of each point were then calculated from the normalized data. The final averages for set I are shown as the measured points in figure 10 with the vertical bars indicating one standard error on each side.

The theoretical curves plotted in figure 10 were calculated on the basis of zeroth-order kinematics—inclusion of first-order effects produced a negligible change. They incorporate the smoothed wave-number data of figure 8 in the conversion of energy to slope. They also were normalized to unity at the same position along the group ray at which the averaged wave slope occurred. It is evident that at large distances along the ray there is a loss of wave energy not accountable by the theory. This point will be returned to below.

The theoretical curves used for set II incorporated first-order iterated kinematics. The maximum deviation from zeroth-order theory encountered was 1·7 % in wave slope. Figure 11 presents the data obtained in set II plotted in the same manner as figure 10. Clearly the agreement between theory and experiment

is much better than in set I, and the inclusion of the interaction terms seems favoured. Figure 12 presents the same data as figure 11 in a somewhat different form. The points shown in the upper diagram of figure 12 are the difference between the measured points and the normalized theory omitting the inter-

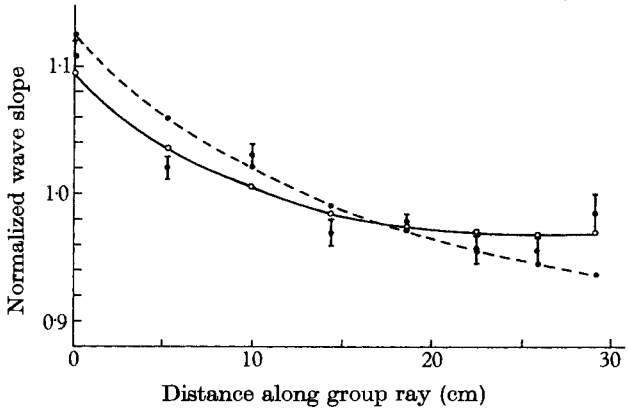

FIGURE 11. Wave slopes in presence of flow—set II (6·00 c/s). ○, Theoretical interaction; ●, theoretical non-interaction; ϕ, measured ± 1 S.E.

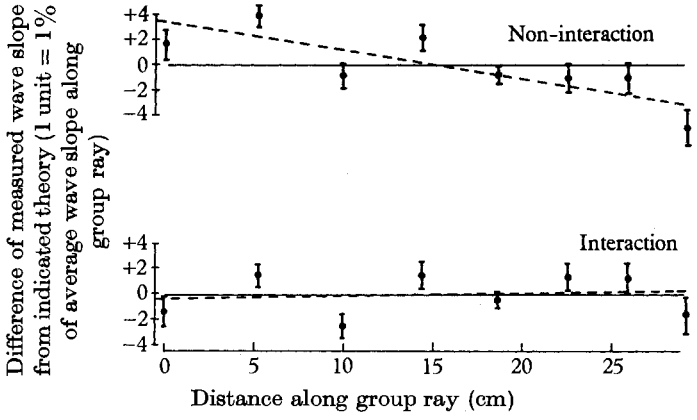

FIGURE 12. Normalized comparisons of theoretical curves with measured wave slopes—set II. – – – –, Least squares regression through measured points; ϕ, measured ± S.D. error.

action term. In the lower diagram of figure 12 the points plotted are this difference including the interaction term. In both cases, the vertical bars indicate one standard error on each side of the points, and the dashed straight line was obtained by least squares regression through the points. The interaction effect resulted in an added energy change of 12 % over the distance examined. As can be seen from the lower diagram of figure 12, the experimental data agrees very well with the theory (including the interaction term), but it appears likely that we have underestimated the standard error somewhat. It should be noted that the 12 % change in energy density produced by the interaction effect is to be compared with a 30 % change due to spreading.

5. Discussion

The optical methods used in this experiment were entirely satisfactory—it is estimated that an accuracy of 0·5 % was achieved in all the optical measurements.

The method used to create the shear flow, though extremely simple and adequate, possessed one major drawback—unsteadiness. Because of upwelling at the inner wall, a region of turbulence existed at the edge of the flow. This region produced most of the random variations of wave properties that were subsequently dealt with by statistical analysis.

Considerable time was spent trying to produce waves with very little transient modulation. Unfortunately, the problem was not entirely solved. The attempt to randomize the phase of the modulation from pulse to pulse appears to have succeeded for set I data but not completely for set II.

It appears that a further experimental investigation is warranted into viscous dissipation and propagation properties of waves near $k = 2{\cdot}7\ \mathrm{cm}^{-1}$ both in the presence and absence of mean flow.

The interaction measurements as presented in figure 10 are definitely anomalous. The difference in decay rate between the measured points and the theoretical curves is in the same sense and of approximately the same magnitude as the discrepancies noted in the viscous decay between 8·57 and 10·0 c/s. It is perhaps significant that a sudden decay of energy occurs very near the position along the group ray, 12 cm, at which $k = 2{\cdot}7\ \mathrm{cm}^{-1}$.

No anomalies were found in the information taken in set II and figures 11 and 12 clearly indicate that interaction theory is well favoured over non-interaction theory.

This work is a contribution of Defence Research Board of Canada. One of us (B. A. H.) was on study leave from the Pacific Naval Laboratory, Esquimalt, the other (R. W. S.) assigned by D. R. B. to special duty at the University of British Columbia. Equipment was purchased from a D.R.B. research grant.

We wish to thank the Department of Civil Engineering, University of British Columbia, for permission to conduct this experiment in the Hydraulics Laboratory.

REFERENCES

Drent, J. 1959 A study of waves in the open ocean and of waves on shear currents. Doctoral Thesis, University of British Columbia.

Johnson, J. W. 1947 *Trans. Amer. Geophys. Un.* **28**, 867.

Lamb, H. 1932 *Hydrodynamics.* 6th edition. Cambridge University Press.

Longuet-Higgins, M. & Stewart, R. W. 1960 *J. Fluid Mech.* **8**, 565.

Longuet-Higgins, M. & Stewart, R. W. 1961 *J. Fluid Mech.* (in the Press).

Pierson, W. J. & Fife, P. 1960 Some properties of long crested periodic waves with lengths near 2·44 centimeters. *Technical Report,* Dept. of Meteorology and Oceanography, Research Div., College of Engng, New York University.

Wilton, J. R. 1915 *Phil. Mag.* **29**, 688.

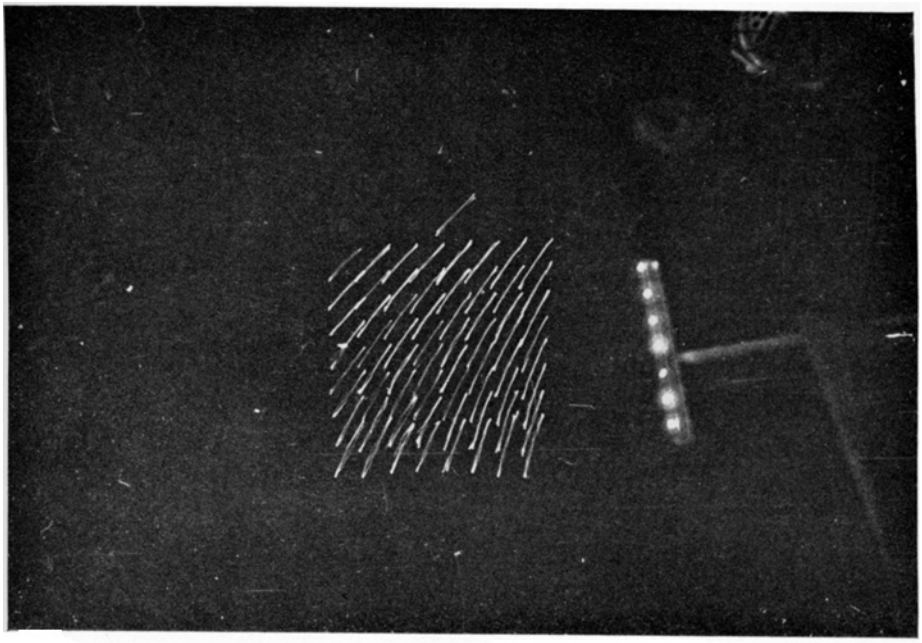

(*a*)

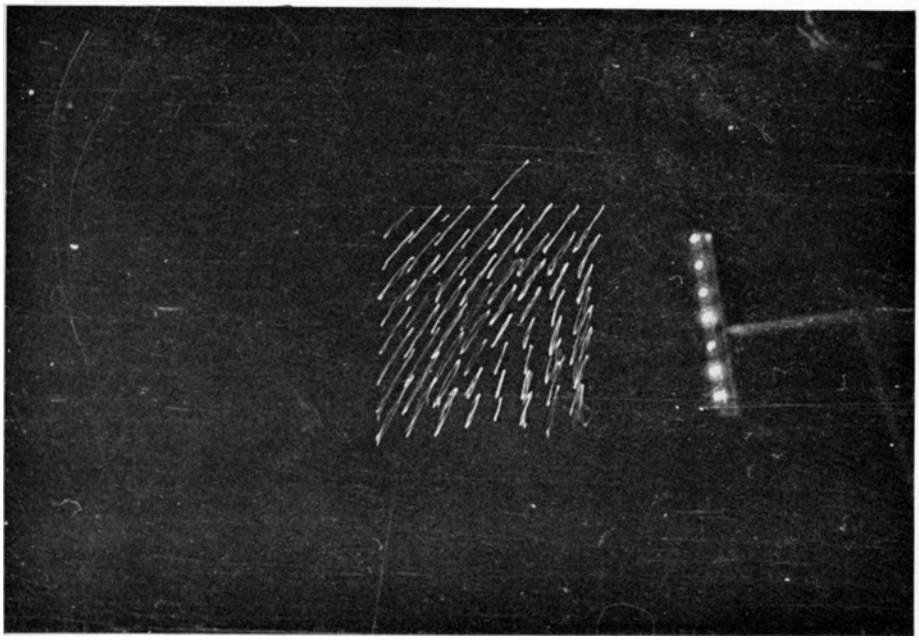

(*b*)

For legend see plate 2.

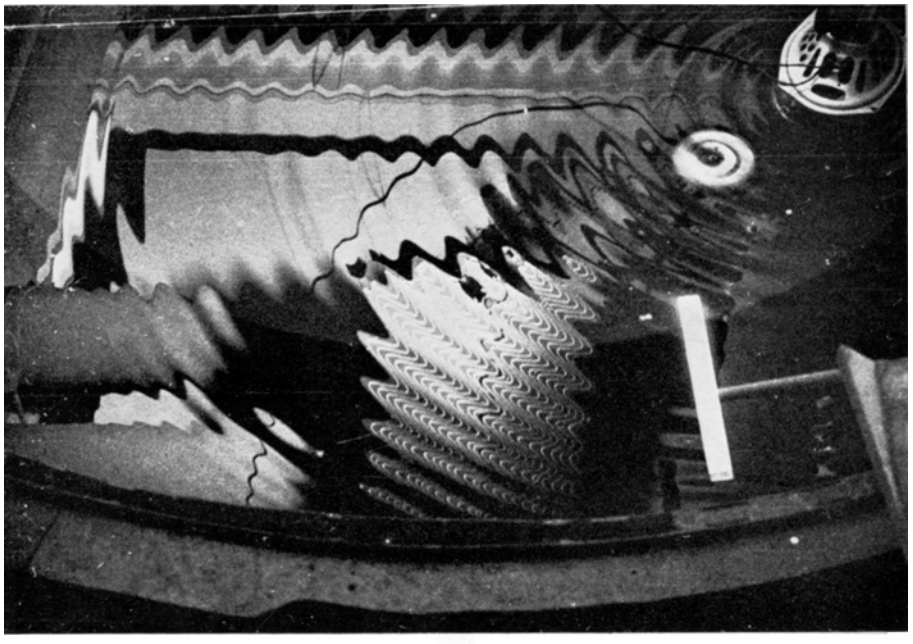

(*c*)

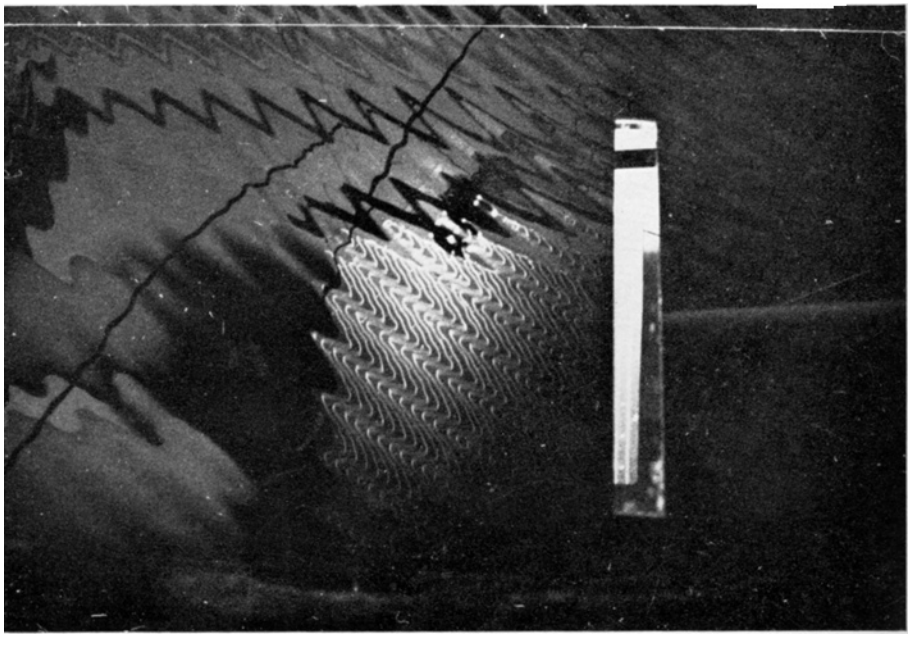

(*d*)

FIGURE 4. (Plates 1 and 2.) (*a*) Selected photograph for the determination of wave amplitudes in the presence of a shear flow (6·00 c/s). (*b*) Rejected wave amplitude photograph (6·00 c/s). (*c*) Wave-number photograph with shear flow (6·00 c/s). (*d*) Wave-number photograph without shear flow (10·5 c/s).